ELSEVIER

Chemical Engineering Journal 91 (2003) 191–198

Chemical Engineering Journal

www.elsevier.com/locate/cej

Catalytic heat generating element for autonomous domestic heating systems

B.N. Lukyanov*, V.A. Kirillov, N.A. Kuzin, M.M. Danilova, A.V. Kulikov, A.B. Shigarov

Boreskov Institute of Catalysis, Pr. Akad. Lavrentieva 5, 630090, Russia

Abstract

New heat-conducting metal porous reinforced catalysts were developed to manufacture a catalytic heat generating element (CHGE) of 25 kW power. The element was subjected to thermophysical, hydraulic and ecological testing. Local temperature and gas flow rates were determined in different places of the outer catalytic bed surface. We have estimated impact of the convective and radiant transfer in total CHGE heat generation. Dynamics of CHGE startup was studied. A prototype of the catalytic water boiler supplied with a CHGE of 25 kW power was manufactured and tested. The boiler provides below yield of toxic waste: CO 5–10 ppm, NO_x traces, CH_4 10–20 ppm, CO_2 10 vol.%, the other gases 89.5 vol.%. CHGE is promising as a device for ecologically safe heat production for household appliances.

Keywords: Catalyst; Combustion of natural gas; Design of the heating element; Generated heat; Water boiler; Ecological parameters

1. Introduction

Hydrocarbon fuels are combusted at temperatures ranging from 1200 to 1500 °C in different flame burners to produce heat energy for industry and household appliances. Because of the ease of flame combustion and high temperature of the combustion products, this method is still the only one used to produce heat in modern times. The main problem, arising on flame combustion of natural gas in air, is formation of NO_x and CO. NO_x result from interaction between nitrogen and oxygen in the most hot part of flame (1800 °C and above). To reduce concentration of toxic components in the combustion products, combustion temperature should be decreased to 900 °C. For this purpose catalytic methods are used [1–3]. Catalytic combustion radically differs from traditional burning, because gas is oxidized on the solid catalyst surface without flame formation [4]. The catalyst permits one to avoid conditions allowing formation of NO_x and to provide more complete conversion of natural gas.

The catalysts for natural gas combustion can be conventionally subdivided into three groups regarding their activity and thermal stability. Thus, palladium catalysts provide gas oxidation at low temperature 500–850 °C and exhibit high activity [3,5–7]. On methane oxidation at temperatures above 900 °C, behavior of the palladium-supported catalysts is rather intricate owing to transformation of PdO into metal Pd. Such transformations lead to large hysteresis in rates of methane combustion [7–9]. Platinum, rhodium, metal oxides Fe_2O_3, Mn_2O_3 etc. are preferable for combustion at moderate temperatures 800–1000 °C [10]. At high temperatures to 1200 °C, hexa-alumina [11–15], perovskites [16] and fibrous ceramic materials [17] are used because of high thermal stability.

The main problem with an application of catalytic fuel oxidation for production of heat in power units is a transfer of heat from the catalyst to the heated working medium. Because of high exothermicity of methane combustion ($\Delta H = -802.3$ kJ/mole), hot spots appear in the first part of the fixed catalyst bed. Modeling the adiabatic reactor with a fixed catalyst layer Ni/Al_2O_3, it was established [18] that the temperature of such "hot spot" may be higher than 1500 °C for $CH_4/O_2 = 1.67$. Different methods for heat removal were proposed for reactors with a fixed catalyst bed by two-step introduction of oxygen [19], catalytic heat generators with a fluidized catalyst bed and built-in heat-exchangers [20,21], reactors with sintered metal bodies covered with highly porous ceramic layers [22], and catalytic burners with an outer water-cooling [23].

A novel method for effective heat removal implies formation of heat generating catalytic systems which are not spatially separated from heat pick-up surfaces. We have previously shown [24,25] that porous metal and reinforced

* Corresponding author. Tel.: +7-383-234-3210; fax: +7-383-234-1187.
E-mail address: lukjanov@catalysis.nsk.su (B.N. Lukyanov).

1385-8947/02/$ – see front matter
PII: S1385-8947(02)00153-5

Nomenclature

Symbols

d	diameter of a hole (m)
D	inner diameter of gas-distributing tube (m)
e	inhomogeneity of gas-distribution along GDT length
F	sum of hole cross sections versus cross section of GDT
g	consumption of gas through a hole ($m^3\,s^{-1}$)
h	perforation pitch (m)
k	coefficient (see Eq. (1))
L	length of the catalyst layer (m)
N	number of holes or heat flow (kW)
P	excess average pressure inside GDT (Pa)
ΔP	pressure drop (mm H_2O)
s	cross section of GDT (m^2)
S	surface area of the catalyst layer (m^2)
ΔT	temperature difference in the layer (area ΔZ) (°C)
U	of gas flow ($m\,s^{-1}$)
ΔZ	length of linear temperature decrease in the layer (m)

Greek symbols

α	coefficient of air excess
ρ	density ($kg\,m^{-3}$)
λ	coefficient of heat-conductivity ($Wt\,m^{-2}\,K^{-1}$)

Indices

ext	related to the outer layer surface
i	a hole number
in	related to the catalyst layer
min	minimal
mix	gas–air mixture
max	maximal
r	radial
-	average

porous metal supports permit one to design new catalytic materials exhibiting high heat-conductivity and providing good heat transfer to the heat carrier.

The aim of the present work is to design a heating element supplied with a reinforced catalyst supported on the porous metal carrier and to test its thermophysical, hydraulic and ecological properties for future application in domestic boilers.

2. Technology for catalyst preparation

The reinforced catalyst is prepared as a porous metal nickel–aluminum or a titanium–aluminum matrix, containing particles of the catalyst active component, supported on the metal net. As catalyst active components, Pd/Al_2O_3 and Pt/Al_2O_3 were used. The catalyst preparation includes the below stages:

- preparation of a charge from metal powders of aluminum, nickel, titanium and its mixing with traditional catalysts Pd/Al_2O_3 or $Pt/\ Al_2O_3$;
- annealing of the reinforced grid;
- preparation of a solution of organic glue and slip;
- deposition of the slip on the reinforced grid, drying and densifying with rollers;
- cutting of bars and their corrugation;
- winding of corrugated and flat plates on the metal structural unit of CHGE and sintering in the vacuum furnace.

The process of sintering of nickel (titanium) and aluminum powders is based on the self-propagating high temperature synthesis of intermetallides [26,27]. Sintering starts at the aluminum melting point (660 °C). The melt quickly spreads over the nickel (titanium) particle surface, which drastically increases the area of component interaction. The process of intermetallide formation accelerates as temperature sharply increases (heat "explosion"). After sintering, the thickness of the catalyst layer is about 0.25 mm on each side of the reinforced grid and its fraction is 60–65 wt.% from the total grid weight. The catalyst has a large porous structure, the main pore volume is built by pores 1.0×10^4–6.0×10^4 nm in radius, the total volume of pores is about 0.12 cm^3/g, the specific surface area is 3 m^2/g, and the size of Pt(Pd) particles is 8(11) Å. For standard sintering regime of the reinforced catalyst, dispersity of both platinum and palladium does not decrease. The catalyst plate is characterized by high mechanical strength, the catalyst is safely bound to the metal grid.

3. Design of the catalytic heating element

Design of CHGE is governed by the required heat power and geometry of the boiler furnace volume. The catalyst bed of CHGE should provide complete gas combustion during one-step at 800–850 °C (not higher) and simultaneous heat removal with the heated liquid. Therefore, the catalyst layer should also play the role of a heat-exchanger. Note that heat removal should not disturb the natural gas oxidation and affect the concentration of NO_x, CO and unreacted methane in the reaction products.

Fig. 1 shows the general view of CHGE meeting the above requirements. The element is built as a ring-type tubular heat-exchanger with an inner gas-distributing tube (GDT) 1. The tube is corrugated and sealed on one side. Natural gas and air are preliminary mixed, then supplied to GDT. Here the mixture leaks through holes in the corrugated side surface of GDT and passes to the intertubular area. The number and diameter of holes are chosen so that the rate of gas flow suction exceed the standard rate of flame propagation on

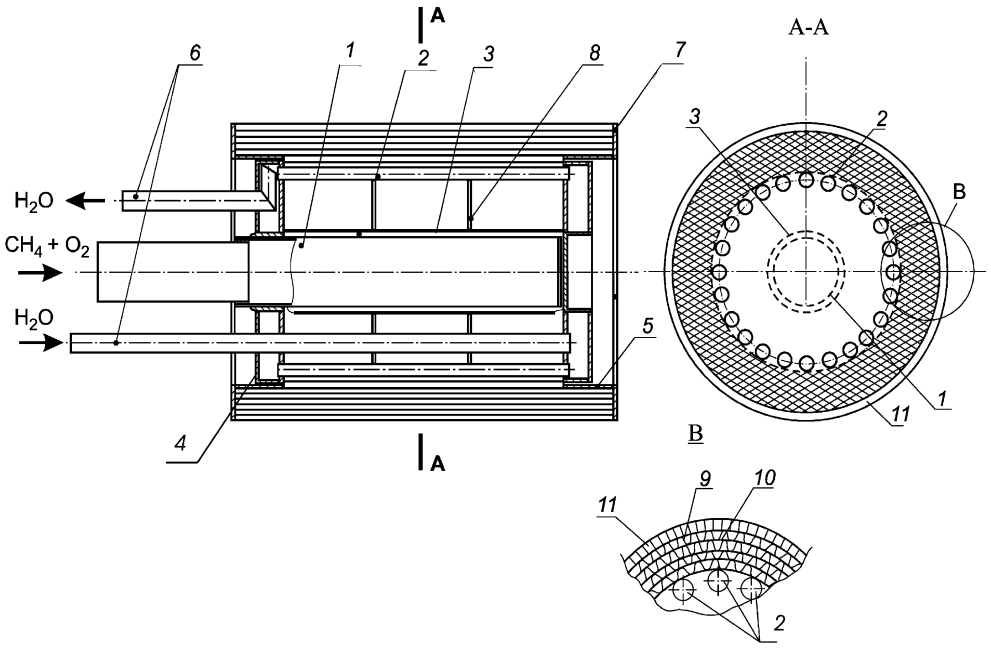

Fig. 1. General view of the catalytic heat generating element of 25 kW power: (1) gas-distributing tube; (2) connection tube of the inner water-cooling heat-exchanger; (3) flow splitter; (4) water header; (5) face ring; (6) downcomers and drain-pipes; (7) flange; (8) stiffening rib; (9) corrugated catalyst plate; (10) flat catalyst plate; (11) startup catalyst layer.

methane combustion in air (0.345 m/s). To suppress the rate of flows leaking through perforation holes, a flow splitter 3 is placed around the gas-distributing tube. On passing the splitter, the gas–air mixture enters the catalyst layer.

The catalyst layer is formed by flat (10) and corrugated (9) catalyst plates wound around the heat-exchanger tubes (2) and sintered. The plates are arranged so that odd rows are formed by corrugated plates, and even rows, by flat plates. The catalyst layer thickness is chosen to allow minimal concentrations of CO, NO_x and unreacted methane in waste gases. The plates form catalytically active channels serving the oxidation of the gas–air mixture on the walls to yield CO_2 and water. The oxidation reaction products are removed through the channel into the environment. The catalyst layer is wider than the tubular heat-exchanger by a value of face rings 5. CHGE is supplied with tubes (6) for feeding cold water and removal of hot water. The element is provided with flanges 7 and stiffening ribs 8. To improve startup of CHGE, the size of corrugation of the outer catalyst layer (11) is larger than that of the underlying layers. Using collectors, the heat-exchanger tubes are united to form a circular cylindrical unit which is supplied with water to be heated. The number of heat-exchanger tubes and their diameter is chosen so that to built a basis for the catalyst layer and to allow minimal pressure drop as water passes through them.

CHGE and its inner water-cooled heat-exchanger are designed for a generated power value of 20–50 kW. For the range of 0.75–10 kW, the heating elements are of a more simple design (see [24,25]).

4. Testing of catalytic heat generating elements

4.1. Hydrodynamic testing

The catalyst layer thickness is about 20 mm, the porosity is 0.8–0.85, the channel size is 1–2 mm, and the rate of filtration is about 0.5 m/s. According to calculations, the pressure drop in such layer can not be significant. Consequently, the catalyst layer can not significantly affect distribution of the gas–air mixture. To provide uniform mixture distribution, a gas-distributing tube should be used.

Distribution of the gas–air mixture is determined by the number and diameter of holes, and perforation pitch. In our experimental tests at normal conditions (“cold tests”) we used gas-distributing tubes 18 and 28 mm in diameter and 300, 400, and 500 mm long (Fig. 2). Assuming that consumption through all holes are equal and taking no account of friction losses, surplus pressure in the gas-distributing tube will be calculated by equation:

$$P = \frac{8\rho Q^2}{\pi^2 N^2 k^2 d^2} \quad (1)$$

The empirical coefficient k, characterizing the stream compressing on suction through a hole, was determined from the experiment. The experimental and calculated data agree if the diameter of gas-distributing tube is 28 mm, $k = 0.60$, the hole diameter is 1.5 mm and the perforation pitch is 20 mm (Fig. 3). As the number of the holes increases, the pressure drop of GDT decreases and not high than 700 Pa if the rated consumption of air is 7.5 l/s.

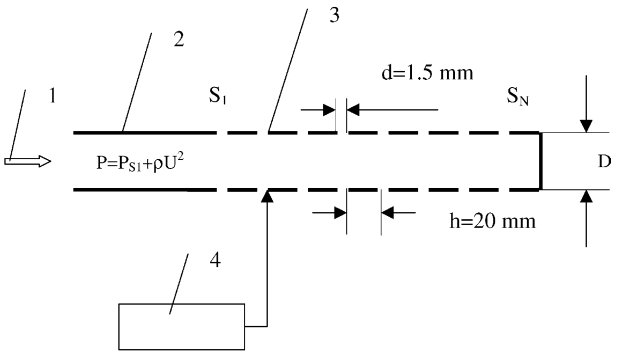

Fig. 2. Scheme of hydraulic tests of gas-distributing tube: (1) gas supply; (2) region of flow stabilization; (3) corrugated part of the tube; (4) pressure gauge.

Measuring the static pressure along the tube, one can determine gas flow rate through each hole q_i and degree of its non-uniform consumption along GDT e:

$$q_i = \frac{\pi d^2}{4} k \sqrt{\frac{2P_i}{\rho}} \tag{2}$$

$$e = \frac{q_{i,\max} - q_{i,\min}}{\bar{q}_i} \tag{3}$$

If pressure profile is monotonic along the tube length, pressure drop is:

$$P_{\max} - P_{\min} = |\Delta P| = |P_N - P_1| \tag{4}$$

If non-uniformity of gas flow rate is not large, the average rate of gas flow through a hole is

$$\bar{q}_i \approx \frac{q_N + q_1}{2} \tag{5}$$

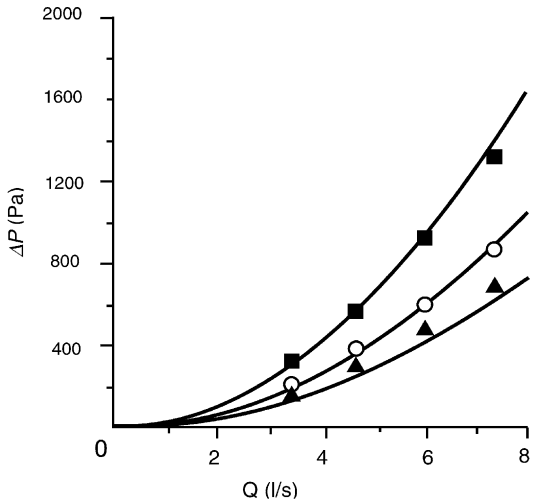

Fig. 3. Pressure drop of the gas-distributing tube versus rate of air flow at standard conditions: $k = 0.60$, $d = 1.55$ mm, $h = 20$ mm, $D = 28$ mm, $L = 400$ mm, (■) $N = 156$; (○) $N = 196$; (▲) $N = 236$; solid line data calculated by Eq. (1).

Then, neglecting friction losses as compared to pressure in GDT and using Eqs. (2)–(5), we have:

$$e \approx 2\frac{\sqrt{P_N} - \sqrt{P_1}}{\sqrt{P_N} + \sqrt{P_1}} = 2\frac{P_N - P_1}{(\sqrt{P_N} + \sqrt{P_1})^2} \approx \frac{|\Delta P|}{2P} \tag{6}$$

Pressure drop along the length ΔP is determined by forces of viscous friction on the wall and dynamic pressure drop due to gas removal with respect to a wall. In this case:

$$\frac{\Delta P}{P} = (kF)^2$$

Then

$$e \approx \frac{(kF)^2}{2} \tag{7}$$

According to Eq. (7), the value of non-uniformity does not practically dependent on gas flow rate, diameter and length of the corrugated part of GDT. Fig. 4 presents the experimental data treated with Eq. (6) and data calculated with Eq. (7). To provide gas flow rate non-uniformity not >5%, the total area of holes should be not <55% from the cross section of GDT.

Pressure drop of CHGE with respect to gas is formed by pressure drop of GDT and the catalyst layer. Fig. 5 presents data on the total resistance with respect to gas of CHGE-25 operating at “cold” and working conditions. The data indicate that at the rated operation regime of CHGE:

- GDT produces the main resistance which is about 30 mm water column;
- catalyst layer increases pressure drop by 16% compared to GDT;
- reaction occurrence increases resistance by approximately 20%.

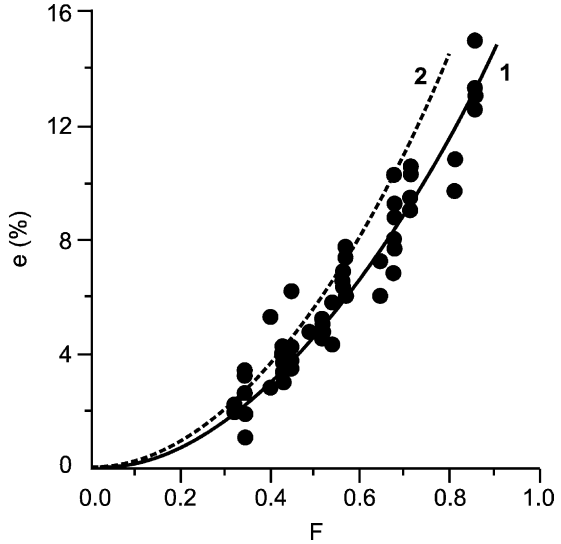

Fig. 4. Non-homogeneous consumption of air versus relation of the total area of holes and cross section of the gas-distributing tube. (●) Experimental data calculated by Eq. (6); (lines) data calculated by Eq. (7): (1) $k = 0.60$, (2) $k = 0.67$.

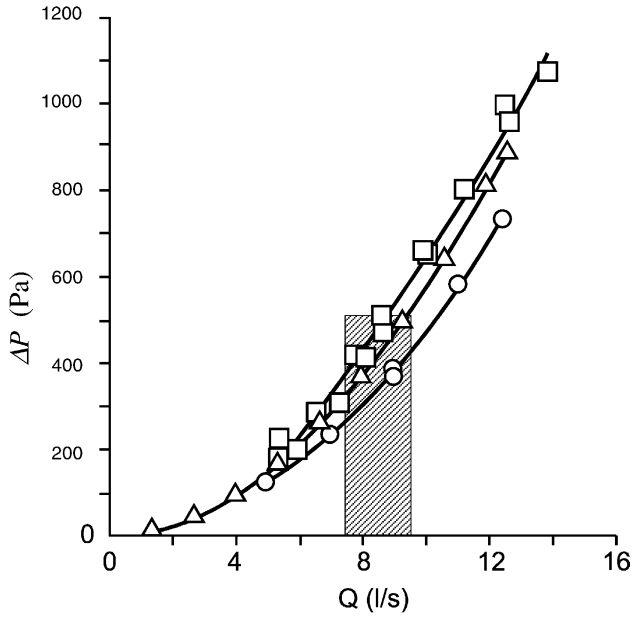

Fig. 5. Pressure drop of CHGE of 25 kW power versus rate of gas air mixture. (O) blowing of the gas-distributing tube with air $Q = 4.9$–12.5 l/s; (Δ) the same in the presence of the catalyst layer at "cold" conditions $Q = 1.3$–12.7 l/s; (□) the same in the presence of the catalyst layer at "hot" conditions $Q = 5.4$–14.0 l/s. The crosshatched rectangle shows the region of the rated operation regime of CHGE of 25 kW power.

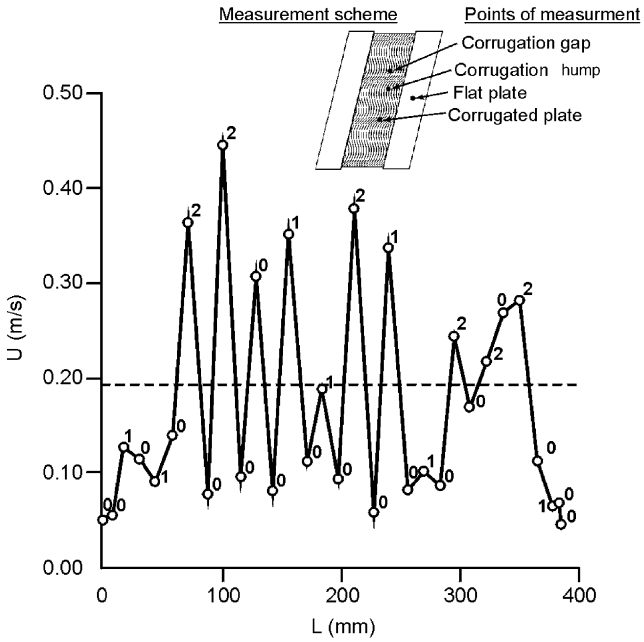

Fig. 6. Distribution of air flow rate at the catalyst layer outlet. The dotted line shows the average suction rate of 0.19 m/s, rate measurements: (0) over the flat plate, (1) between flat plates (corrugation gap), (2) between flat plates (corrugation hump).

To determine the effect of catalyst layer winding on the distribution of the gas–air mixture flow velocity near the outer catalyst layer surface of CHGE using the thermoanemometry method. We have studied local suction rates in different places of the outer catalyst layer surface of CHGE of 25 kW power. If the average suction rate is 0.19 m/s, there are rate fluctuations over the catalyst layer surface, moreover, the rates of flow differ in different points by more than a factor of 2 (Fig. 6).

4.2. Thermal physical testing

Local temperature of the outer catalyst layer surface was measured with four fixed thermocouples placed between the outer flat plate and a corrugated one. CHGE was horizontally placed in a water-cooled jacket during testing. The thermocouples were installed 65, 150, 285, and 395 mm from the inner face. The catalyst layer was 410 mm long. Temperature of inlet and outlet water of the inner water-cooled heat-exchanger were measured at a time. Measuring was performed at the steady-state regime and generated power was ranged from 16 to 30 kW. Table 1 presents temperature data.

As Table 1 suggests, the maximal temperature difference is 61 °C on the outer catalyst layer surface of CHGE. Moreover, we have visually observed red-hot (~40%) and less heated (60%) catalyst plates on the outer catalyst surface.

To measure temperature profile across the catalyst layer thickness, we made a channel at 45° to the surface and placed a movable thermocouple into it. The channel was made at 1/3 of layer length from the CHGE face. Temperature was measured at the rated operation regime of CHGE that is at 25 kW power (Fig. 7). The temperature profile has the maximum in the middle of the layer. Low temperature values at the beginning of the profile are associated with cooling of the gas–air mixture by the inner heat-exchanger. A temperature decrease in the region nearing the outer layer surface is associated with outer heat-exchange and complete methane combustion.

The temperature profile across the layer thickness permits one to estimate the coefficient of radial heat-conductivity λ_r. The fact that temperature decreases almost linearly as the outer surface is approached indicates that the reaction does not occur in this layer region and heat flows at the expense of radial heat-conductivity. This heat flow is removed from

Table 1
Local temperatures of the outer catalyst layer and inner water-cooled heat-exchanger of CHGE-25 on varying generated heat power.

Thermocouple readings (°C)						Capacity CHGE (kW)
No. 1	No. 2	No. 3	No. 4	Inlet H_2O	Outlet H_2O	
792	836	803	792	9.9	55.0	30.3
814	781	814	753	11	58.3	30.0
759	726	759	715	11	51.7	23.6
770	737	759	715	11	48.4	23.6
737	781	748	748	9.9	41.8	23.1
726	704	715	671	11	38.5	19.0
682	649	505	627	11	27.5	16.0
671	649	594	627	11	47.3	16.0

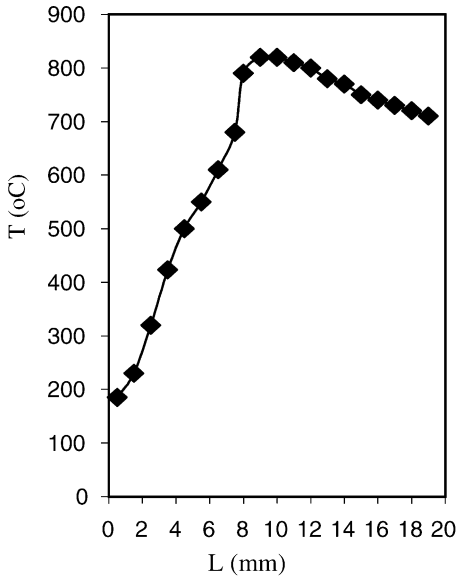

Fig. 7. Distribution of temperature across thickness of the catalyst layer of CHGE operating at rated operation regime. (■) experiment: $Q_{mix} = 8.3$ l/s, $\alpha = 1.22$, water consumption in the heat-exchanger of CHGE $Q_{H_2O} = 69.5$ g/s.

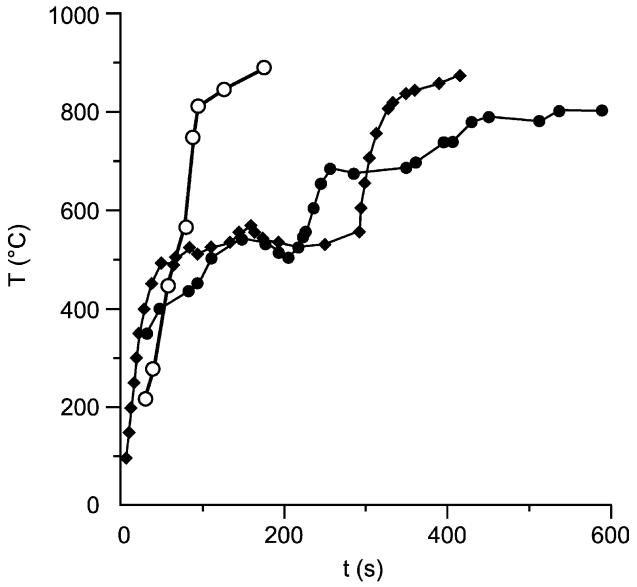

Fig. 8. Heating of the catalyst layer of CHGE by firing the gas–air mixture. Flow rates: (●) methane 0.084 l/s, air 0.44–0.96 l/s, (◆) flow rates of methane 0.084 l/s and air 0.96 l/s, (○) flow rates of methane 0.084 l/s and air 0.96 l/s if two startup layers are used.

the outer surface by convection and radiation. Then we have:

$$\lambda_r = \frac{N_{ext}\Delta Z}{S_{ext}\Delta T_{in}} = \frac{7.2 \times 10^3 \times 5 \times 10^{-3}}{0.232 \times 100} = 1.55 \quad (8)$$

Thus, generated power is removed by the inner heat-exchanger of CHGE from the inner catalyst layer surface and by radiation, convection and with heat of waste gas from the outer surface. On varying the generated heat power from 16 to 30 kW, the density of surface heat flux increases from 69 to 129 kW/m^2. Based on the heat balance of CHGE, we calculated the fractions of generated power which are removed through different mechanism of heat transfer (see Table 2).

4.3. Dynamics of CHGE startup

A choice of the catalyst layer heating method determines the startup time which is the most important characteristic of CHGE. By startup time is meant the time required for heating the catalyst layer to the temperature of methane oxidation with air oxygen. The catalyst layer can be heated from the outside or inside. The outside heating is performed by flame formed on burning of the methane–air mixture which flows from the layer. The inside heating can result from exothermal reaction accompanied by large heat effect. Both methods were experimentally investigated. The outer surface layer heating was chosen because of its simplicity. Dynamics of the catalyst layer startup is shown in Fig. 8. For the rated air excess ($\alpha = 1.1$), the time of startup of CHGE-25 into operation is about 300 s. Using two startup layers on the outer catalyst layer (Fig. 1), the startup time was reduced to 90 s.

Table 2
Fractions of generated power removed from CHGE

	Power (kW)	Fraction (%)
Heat removal to water of CHGE heat-exchanger	9.2	36.7
Heat removal with waste gases	7.0	28.1
Heat removal by convection and radiation	8.8	35.2
Total heat power of CHGE	25	100

4.4. Ecological testing

CHGE was subjected to long and short-term testing. In the course of short-term testing, the below parameters were monitored: temperature, pressure, consumption of natural gas, water and air, and composition of waste gases. On combustion of line natural gas, containing (vol.%) methane-97.46, ethane-1.11, propane-0.37, isobutane-0.06, butane-0.06, and pentane-0.02, waste gases contained: CO 5–10 ppm, NO_x traces, CH_4 10–20 ppm, CO_2 10 vol.%, the rest gases (N_2, O_2) 89.5 vol.%. According to long-term testing (1000 h), the catalyst preserves its activity and the initial ecological parameters of CHGE do not change (Fig. 9).

4.5. Testing of CHGE-25 as a part of the water boiler

A catalytic heat generating element of 25 kW power was used for heat generation in the boiler prototype. Testing was performed on the technological bench. The bench permitted one to perform testing of the whole water boiler and its units such as: a combustion chamber, a heat-exchanger, a blowing unit, a mixing chamber, a heat-exchanger of operation water

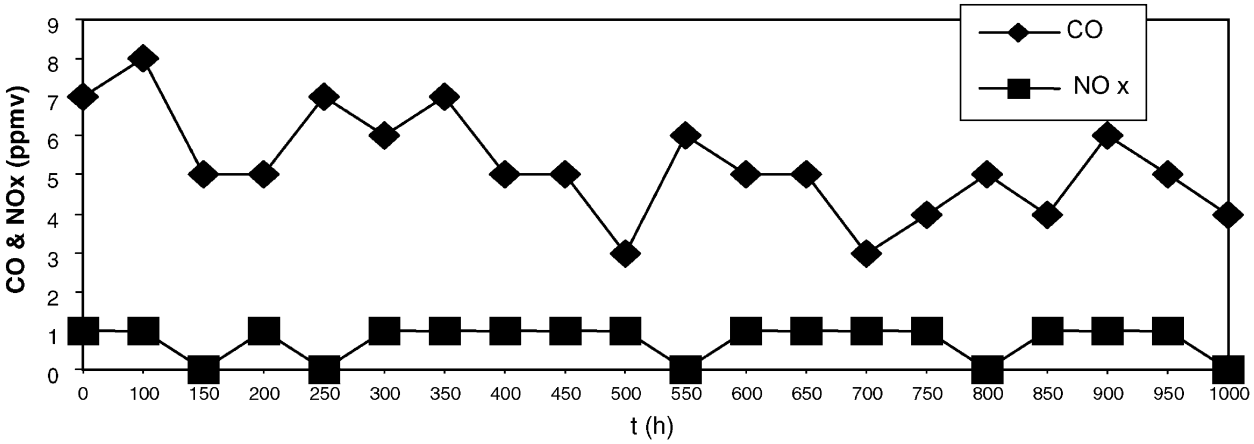

Fig. 9. Concentrations of CO and NO_x in waste gases from CHGE operating at the design regime (long-term testing).

Table 3
Testing of the gas catalytic boiler based on the CHGE of 25 kW power

Parameters	Data
Rated consumption (m^3/h) of	
Natural gas	2.46
Gas–air mixture	29.52
Temperature (°C) of	
Catalyst surface	830
Waste gases	110
Water at heat-exchanger inlet	70
Temperature (°C) at	
Outlet from heat-exchanger of CHGE	90
Inlet of preliminary heat-exchanger of boiler	46.5
Outlet from preliminary heat-exchanger of boiler	70
Output of operation water heating (not lower than) (l/min)	
On heating by 35 °C	9
Emission of waste gas (mg/m^3)	
CO	2.2
NO_x	Not observed
Methane	~15
Rated boiler capacity (kW)	24.73
Weight (kg)	70
Efficiency of boiler (%)	96

and control and safety control system units. Some testing data are given in Table 3. The data indicate that the boiler is efficient and ecologically safe.

5. Conclusions

1. The technology for preparation of reinforced catalysts based on the platinum group metals was developed. The technology includes the below stages: preparation of charge, deposition of the charge on the metal grid and sintering, thermal treatment, winding of catalyst plates on the heat-exchanger of CHGE.
2. Hydrodynamic tests of CHGE regarding the distribution of the methane–air mixture were performed. To provide five percent inhomogeneity of gas-distribution, the total area of holes for gas suction in the gas-distributing tube of CHGE should be 0.55 from its cross section. Thermal anemometers were used to measure local rates of the flow emerging from the outer surface of the catalyst layer. At different places, the rates may differ by a factor of 2. Pressure drops of CHGE of 25 kW power measured with respect to gas and water are, respectively 50 and 700 mm water column.
3. Local temperatures were measured in different places of the outer catalyst layer surface and across the layer thickness from the outer surface to the inner heat-exchanger. On the outer surface, the temperature inhomogeneity is about 60 °C. The local temperature maximum is above 800 °C in the catalyst layer depth.
4. We have determined the fractions of generated heat which are removed with water of the inner heat-exchanger (36.7%), waste gases (28.1%), and convection and radiation (35.2%).
5. Different methods for preliminary heating of the catalyst layer and dynamics of startup were studied. The startup time of CHGE-25 with two updated startup layers is about 90 s.
6. The boiler was tested using CHGE of 25 kW power as a heating center. The emission of CHGE is: CO 5–10 ppm, NO_x traces, CH_4 10–20 ppm, CO_2 10 vol.%. The catalytic heating element is very promising for application in water boilers.

Acknowledgements

The authors gratefully acknowledge the financial support of the International Science and Technology Center (ISTC Grant No 763) and fruitful cooperation with Dr. Kuzmin V.A. and Onufriev I.A. in testing of CHGE.

References

[1] D.L. Trimm, Catalytic combustion (review), Appl. Catal. 7 (1983) 249.

[2] A. Nishino, Household appliances using catalysis, Catal. Today 10 (1991) 107.

[3] M.F.M. Zwinkels, S.G. Jaras, P.G. Menon, Catalytic materials for high-temperature combustion, Catal. Rev. Sci. Eng. 35 (1993) 319.

[4] G.K. Boreskov, Heterogeneous Catalysis, Nauka, Moscow, 1986.

[5] R.B. Anderson, K.C. Stein, J.J. Feenan, L.E.J. Hofer, Catalytic oxidation of methane, Ind. Eng. Chem. 53 (1961) 809.

[6] K. Sekizawa, M. Machuda, K. Eguchi, H. Arai, Catalytic properties of Pd-supported hexaaluminate catalysts for high-temperature catalytic combustion, J. Catal. 142 (1993) 655.

[7] R.J. Farrauto, M.C. Hobson, T. Kennelly, E.M. Waterman, Catalytic chemistry of supported palladium for combustion of methane, Appl. Catal. A: Gen. 81 (1992) 227.

[8] P. Salomonsson, S. Johansson, B. Kasemo, Methane oxidation over PdO_x—on the mechanism for the hysteresis in activity and oxygen content, Catal. Lett. 33 (1/2) (1995) 1.

[9] J.G. McCarty, Kinetics of PdO combustion catalysis, Catal. Today. 26 (3/4) (1995) 283.

[10] G.K. Boreskov, Mechanism of oxidation on the solid oxide catalysts, Kinet. Katal. 14 (1973) 2.

[11] M. Machida, K. Eguchi, H. Arai, Catalytic properties of Ba $MA1_{ll}$ $O_{19\text{-}\alpha}$ (M = Cr, Mn, Fe, Co, and Ni) for high-temperature catalytic combustion, J. Catal. 120 (1989) 377.

[12] M. Machida, K. Eguchi, H. Arai, Effect of structural modification on the catalytic property of Mn-substituted hexaaluminates, J. Catal. 123 (1990) 477.

[13] J.G. McCarty, H. Wise, Perovskite catalysts for methane combustion, Catal. Today 8 (1990) 31.

[14] P. Salomonsson, T. Griffin, B. Kasemo, Oxygen desorption and oxidation–reduction kinetics with methane and carbon monoxide over perovskite type metal oxide catalysts, Appl. Catal. A Gen. 104 (2) (1993) 175.

[15] G. Groppi, C. Cristiani, P. Forzatti, F. Breti, S. Mallogi, High temperature combustion of methane over hexaaluminate-supported Pd catalysts, natural gas conversion V, Studies Surface Catal. 5 (1998) 71.

[16] F.M. Ortega, C. Batiot, J. Barrault, M. Granne, J.M. Tatibouet, Catalytic Methane Combustion on La-based Perovskite Type Catalysts, Natural Gas Conversion V, Studies Surface Catal. 5 (1998) 45.

[17] Z.R. Ismagilov, R.A. Shkrabina, T.V. Christyachenko, V.A. Ushakov, N.A. Rudina, Preparation and study of thermally and mechanically stable ceramic fiber based catalysts for gas combustion, natural gas conversion V, Studies Surface Catal. 5 (1998) 83.

[18] A.M. Groote, G.F. Froment, Simulation of the catalytic partial oxidation of methane to synthesis gas, Appl. Catal. A Gen. 138 (1996) 245.

[19] P. Zhi-yong, D. Chao-yang, S. Shi-kong, New two-stage process for catalytic oxidation of methane to synthesis gas, Ranliao Huaxue Xuebao. 28 (4) (2000) 348.

[20] Z.R. Ismagilov, M.A. Kerzhentsev, Catalytic fuel combustion. A way of reducing emission of nitrogen oxides, Catal. Rev. Sci. Eng. 32 (1–2) (1990) 51.

[21] Z.R. Ismagilov, M.A. Kerzhentsev, Fluidized bed catalytic combustion, Catal. Today 47 (1999) 339.

[22] J.C. van Giezen, M. Intven, M.D. Meijer, J.W. Geus, A. Mulder, G.J. Riphagen, J.P. Brouwer, The development of novel metal-based combustion catalysts, Catal. Today 47 (1–4) (1999) 191.

[23] B. Emonts, P. Brockerhoff, Low-emission natural gas combustion in catalytic heater, Proceedings of First European Conference on Small Burner Technology and Heating Equipment, Zurich, 25–26 September 1996, p. 119.

[24] V.A. Kirillov, N.A. Kuzin, V.A. Kuzmin, A.V. Kulikov, A.B. Shigarov, Deep oxidation of hydrogen and hydrocarbon gases on the catalytic heat generating elements, Khim. Prom-st 5 (1994) 332.

[25] V.A. Kirillov, N.A. Kuzin, A.V. Kulikov, Application of catalytic oxidation of hydrocarbon gases for production of heat in domestic needs, Teploenergetika 1 (2000) 18.

[26] Yu.S. Naiborodenko, V.I. Itin, Study of the process of gas-free combustion of powders of different metals. Part 1. Regulations and mechanism of combustion, Fizika Goreniya i Vzryva 11 (3) (1975) 343.

[27] A.P. Savitskii, L.S. Martsunova, N.N. Burtsev, M.A. Yemel'yanova, V.V. Zhdanov, Formation of intermetallides on interaction between solid and liquid phases, Izv. Akad. Nauk SSSR, Metals 2 (1985) 191.